

Integrated Codes for ICRF-Edge Plasma Interactions

D. A. D'Ippolito, J. R. Myra and D. A. Russell

Lodestar Research Corporation, 2400 Central Avenue, Boulder, Colorado

M. D. Carter

Oak Ridge National Laboratory, Oak Ridge, Tennessee

April, 2005

*Presented at the 16th Topical Conference on Radio Frequency Power in Plasmas,
Park City, Utah, April 11-13, 2005*

DOE/ER/86216-1

LRC-05-104

LODESTAR RESEARCH CORPORATION
2400 Central Avenue, Boulder, Colorado 80301

Integrated Codes for ICRF-Edge Plasma Interactions

D.A. D'Ippolito,¹ J. R. Myra,¹ D. A. Russell,¹ and M. D. Carter,²

¹*Lodestar Research Corporation, Boulder, Colorado;* ²*ORNL, Oak Ridge, Tennessee*

Abstract. Progress towards a suite of integrated codes for computing the mutual interaction of ICRF antennas with the turbulent scrape-off-layer (SOL) plasma is described. The rf waves are calculated by the 2D MORRFIC antenna code, modified to include a vacuum sheath boundary condition; the SOL profiles are evolved using the SOLT 2D turbulence code, modified to include nonlinear sheath and ponderomotive physics. The SOLT code includes the physics of 2D turbulence, blob transport, rf convection, and ponderomotive density depletion. Iteration of these codes to convergence would provide self-consistent solutions for the density and the rf waves. Finally, an rf sheath boundary condition is described, which permits an iterative solution for rf fields at the boundary and the associated sheath potential and sheath power dissipation. Physics results and future plans for code integration are discussed.

Keywords: ICRF, rf sheath convection, ponderomotive effects, SOL turbulence and transport

PACS: 52.50.Qt, 52.40.Fd, 52.40.Kh, 52.35.Mw, 52.35.Ra

INTRODUCTION

An outstanding problem in ICRF modeling is to make quantitative predictions of nonlinear ICRF antenna-plasma interactions, including rf sheath, ponderomotive force (PF) and parametric decay effects. (A review of these effects and their importance is given in Ref. [1].) Accurate estimates of these effects require a self-consistent treatment of the rf waves and the plasma. For example, predicting antenna loading, local rf fields, and sheath interactions requires a knowledge of the SOL density profile and the particle flux to the antenna, but the density profile is strongly influenced by nonlinear rf effects such as rf-sheath-induced convection [2] and ponderomotive density expulsion [3]. The density profile can also be strongly affected by turbulence and blob transport (as reviewed in Ref. [4]). Thus, a quantitative study should include the mutual interactions of linear and nonlinear ICRF physics with SOL turbulence, including scattering of ICRF waves off turbulent density fluctuations (blobs), and the effect of the rf-induced sheared flow layers and currents on the underlying turbulence.

The goal of the present work is to develop an integrated suite of 2D codes for making quantitative prediction of ICRF antenna-plasma interactions and for studying the interplay between rf waves and SOL turbulence. The rf fields launched by the antenna are computed by the 2D antenna code MORRFIC [5]. This code can be run in (x,z) geometry (here, x,y,z refer to the radial, poloidal, and toroidal directions) to compute the sheath voltage $V_{sh}(x,y)$ at the boundaries or the ponderomotive potential $\Psi(x,y,z)$ along each field line. The poloidal dependence is included by summing over poloidal harmonics of the antenna spectrum. In (x,y) geometry, the code can

investigate wave scattering off a turbulent density distribution $n(x,y)$ [5]. The SOL profiles are computed by the Scrape-Off-Layer Turbulence (SOLT) code, originally developed to study turbulent blob transport [6], but now modified to include the nonlinear rf physics. The density $n(x,y)$ from SOLT, and the rf fields and the nonlinear rf terms from MORRFIC, can be iterated to obtain a self-consistent solution. This has been tested by hand and will be automated in the next stage of code development.

SOL PHYSICS

The physics of the SOLT code is illustrated by the following vorticity equation:

$$\frac{d}{dt} \left(\frac{nmc^2}{B^2} \nabla_{\perp}^2 \Phi \right) = \nabla_{\parallel} J_{\parallel} + \frac{2c}{B} \mathbf{b} \times \boldsymbol{\kappa} \cdot \nabla p + \frac{c}{B} \mathbf{b} \cdot \nabla \times \mathbf{F}, \quad (1)$$

where $d/dt = \partial/\partial t + \mathbf{v} \cdot \nabla$. (In our 2D SOL model, this equation must be averaged along the field lines.) The first term is the divergence of the ion polarization current, important in describing rf-sheath-driven convection [2]. The next term is the divergence of the parallel current. Integrated along the field line and matched to the dc sheath boundary condition (BC) ensuring quasineutrality, this term becomes [7]

$$\frac{\langle J_{\parallel} \rangle}{nec_s} = 1 - \nu e^{-e\Phi/T} I_0(\xi) \quad (2)$$

where $\langle Q \rangle$ denotes the field-line average of Q , $\nu = (m_i/2\pi m_e)^{1/2}$, $\xi = ZeV_{sh}/T$, and $T \equiv T_e$. The ‘‘rectified potential’’ Φ_0 of 1D sheath theory is obtained by setting $\langle J_{\parallel} \rangle = 0$ to obtain $\exp(\Phi_0/T) = \nu I_0(\xi)$. In our SOL simulations, the rf convection is driven by setting $\Phi = \Phi_0$ at the antenna. Here, $V_{sh}(x,y)$ can be an analytic function (see [2]) or the MORRFIC code result. Equation (2) allows a smooth transition from the rf sheath regime ($\xi \gg 1$) near the antenna to the Bohm sheath regime ($\xi \sim 1$) in the turbulent zone. The third term in Eq. (1) is the curvature drive for the instabilities that drive the turbulence. The saturated turbulence produces 2D ‘‘blobs’’ (or filaments along \mathbf{B}) of enhanced density, which convect outwards at a velocity $\mathbf{v} = c\mathbf{b} \times \nabla \Phi / B$ determined by the vorticity equation [4]. The final term in Eq. (1) describes the drift current due to an external force $\mathbf{F} = \mathbf{F}_i + \mathbf{F}_e$ (e.g. the PF and neutral frictional forces).

In general, the charge balance in Eq. (1) must be supplemented by equations for conservation of particles, energy, parallel current and momentum. In the simplest system (considered here), only conservation of charge, particles and energy are considered, but more complete models can be treated by the same algorithms. To include PF density expulsion, one can solve the parallel momentum equation analytically in the limit of isothermal temperatures and rapid parallel electron motion past the antenna (compared to other time scales) to obtain

$$n = n_0 \exp[-\Psi/(T_e + T_i)], \quad (3)$$

where $\Psi = m_e (e|E_{\parallel}|/2m_e\omega)^2$ is the ponderomotive potential calculated in the MORRFIC code. PF physics has not yet been implemented in the SOLT code.

The SOLT-MORRFIC code suite was tested for a model of the C-Mod antenna, including the poloidal limiters (PL), bumper tiles (BT) and Faraday screen (FS). The

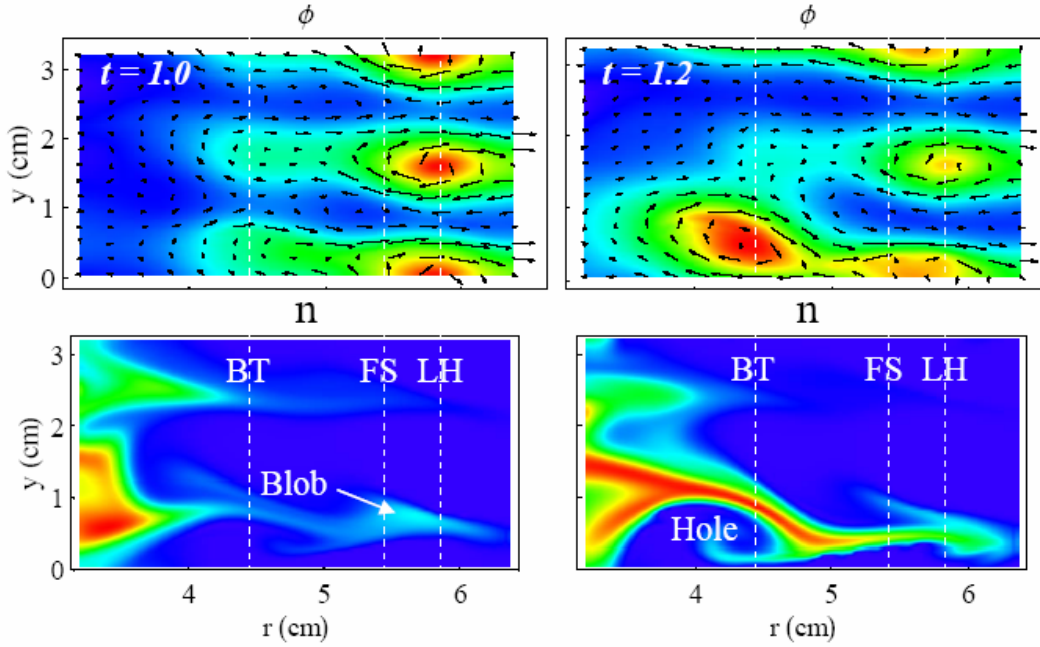


FIGURE 1. Snap-shots of electrostatic potential ϕ and plasma density n as functions of radial and poloidal variables, r and y respectively, from the SOLT simulation based on the MORRIFIC sheath potential calculated after one iteration. LH denotes the lower hybrid resonance, based on the initial density profile. Arrows denoting the convecting $\mathbf{E} \times \mathbf{B}$ velocity overlay the ϕ plot, where $\mathbf{E} = -\nabla\phi$. The notation in the figure differs slightly from the text: $\phi \equiv \Phi$ and $r \equiv x$.

edge and SOL plasmas were modeled with a particle source inside the separatrix and a particle sink BC ($n \rightarrow 0$) well inside the antenna box. The numerical algorithm and detailed BCs will be discussed elsewhere. A single iteration of the codes by hand showed that (i) the equilibrium density and sheath voltage profiles changed significantly in one iteration step, and (ii) the rf convection significantly flattened the density profile in front of the antenna. Shown in Fig. 1 is a blow-up of the SOLT solution for the instantaneous $n(x,y,t)$ and $\Phi(x,y,t)$ in the region near the antenna. The density plot shows the existence of coherent propagating density maxima (blobs) and minima (holes), and the potential plots show the rf convective cell structure near the antenna. Notice the pronounced convection of the density blob into canals between the isolated vorticity cells associated with the lower hybrid resonance. Also note the large vorticity cell shed by the antenna, correlated with a density depression or hole. This figure illustrates the complex interplay between rf and turbulence that can be studied with this suite of codes.

RF SHEATH BC

Rf sheaths can substantially modify the rf fields near the boundaries. Most antenna codes or full-wave codes do not include this physics and use simple conducting wall BCs to compute the rf fields. The MORRIFIC code models the sheaths as thin vacuum regions near the boundaries [5]. In MORRIFIC, the sheath voltage V_{sh} is calculated by

integrating E_{\parallel} across the vacuum layer. However, this approach requires good grid point resolution near the boundaries and can lead to numerical instabilities. To solve this problem, we have recently derived an analytic rf sheath BC generalizing the Appendix of Ref. [8]:

$$\nabla_t \cdot \mathbf{E}_t - \frac{\Delta}{1+i\nu} \nabla_t^2 D_z = 0, \quad B_z = 0. \quad (4)$$

The first relation is a jump condition expressing $\nabla \cdot \mathbf{D} = 0$ across a thin electrostatic sheath layer with dielectric constant $\epsilon_{zz} = 1+i\nu$, where z is the direction normal to the sheath and t denotes the tangential component. Here, the fields \mathbf{E} , \mathbf{B} and \mathbf{D} are defined on the plasma side of the sheath-plasma interface, and Δ is the time-averaged sheath width (which is related to the sheath capacitance). In the limit $\Delta \rightarrow 0$ the usual conducting wall BC ($E_t = 0$) is recovered. The sheath voltage and width are related by

$$V_{\text{sh}} \equiv \int_{z=0}^{\Delta} dz E_z^{(\text{sh})} \approx \frac{D_z \Delta}{1+i\nu}, \quad \Delta = \lambda_D \left(\frac{eV_{\text{sh}}}{T_e} \right)^{3/4}, \quad (5)$$

where $E_z^{(\text{sh})}$ and D_z are the defined at the sheath and plasma sides of the boundary, respectively. These relations imply the nonlinear scaling $\Delta \sim E_z^3$. Finally, the sheath dissipation parameter $\nu \equiv \text{Im}(\epsilon_{zz})$ is defined as

$$\nu = \frac{4\pi\Delta}{\omega V_{\text{sh}}^2} \left(\frac{P_{\text{sh}}}{A} \right), \quad \frac{P_{\text{sh}}}{A} \equiv n_e c_s T_e \xi h(\xi) \frac{I_1(\xi)}{I_0(\xi)}, \quad (6)$$

where $\xi = ZeV/T_e$, $h(\xi) = (0.5 + 0.3 \xi)/(1 + \xi)$ is a form factor connecting known results in the limits $\xi \ll 1$ and $\xi \gg 1$, and P_{sh} is the sheath power dissipation [7] (the flux of ions into the sheath \times the ion energy gain in the sheath). An rf field solution incorporating Eqs. (4) - (6) can be iterated to obtain a self-consistent solution for the rf fields, sheath voltage, and power dissipation. Note that this procedure gives the local distribution of the sheath effects on material surfaces, so that problem locations (e.g. ‘‘hot spots’’) can be identified, as well as global quantities computed (e.g. total sheath power dissipation). A related BC has been considered for plasma processing [9]. It is planned to test our sheath iteration procedure in both antenna and full-wave codes.

ACKNOWLEDGMENTS

This work was supported by US DOE grants DE-FG02-04ER86216 and DE-FG03-97ER54392.

REFERENCES

1. Myra, J.R., D’Ippolito, D.A., Russell, D.A., Berry, L.A., *et al.*, this conference.
2. D’Ippolito, D.A., Myra, J.R., Jacquinet, J., and Bures, M., *Phys. Fluids B* **5**, 3603 (1993).
3. Motz, H., and Watson, C.J.H., *Adv. Electron.* **23**, 153 (1967).
4. D’Ippolito, D.A., Myra, J.R., Krasheninnikov, S.I., *et al.*, *Contrib. Plasma Phys.* **44**, 205 (2004).
5. Carter, M.D., D’Ippolito, D.A., Myra, J.R., Russell, D.A., this conference.
6. Russell, D.A., D’Ippolito, D.A., and Myra, J.R., *Bull. APS* **49** (2004), paper CP1.066.
7. D’Ippolito, D.A., and Myra, J.R., *Phys. Plasmas* **3**, 420 (1996).
8. Myra, J.R., D’Ippolito, D.A., and Bures, M., *Phys. Plasmas* **1**, 2890 (1994).
9. Jaeger, E.F., Berry, L.A., Tolliver, J.S., and Batchelor, D.B., *Phys. Plasmas* **2**, 2597 (1995).